



## **Sparse Automotive MIMO Radar for Super-Resolution Single Snapshot DOA Estimation With Mutual Coupling**

Downloaded from: <https://research.chalmers.se>, 2024-04-20 16:14 UTC

Citation for the original published paper (version of record):

Amani, N., Jansen, F., Filippi, A. et al (2021). Sparse Automotive MIMO Radar for Super-Resolution Single Snapshot DOA Estimation With Mutual Coupling. IEEE Access, 9: 146822-146829. <http://dx.doi.org/10.1109/ACCESS.2021.3122967>

N.B. When citing this work, cite the original published paper.

© 2021 IEEE. Personal use of this material is permitted. Permission from IEEE must be obtained for all other uses, in any current or future media, including reprinting/republishing this material for advertising or promotional purposes, or reuse of any copyrighted component of this work in other works.

Received August 25, 2021, accepted October 14, 2021, date of publication October 26, 2021, date of current version November 4, 2021.

Digital Object Identifier 10.1109/ACCESS.2021.3122967

# Sparse Automotive MIMO Radar for Super-Resolution Single Snapshot DOA Estimation With Mutual Coupling

NAVID AMANI<sup>1,2</sup>, FEIKE JANSEN<sup>3</sup>, ALESSIO FILIPPI<sup>3</sup>, (Member, IEEE),  
MARIANNA V. IVASHINA<sup>1</sup>, (Senior Member, IEEE),  
AND ROB MAASKANT<sup>1,2</sup>, (Senior Member, IEEE)

<sup>1</sup>Department of Electrical Engineering, Chalmers University of Technology, 412 96 Gothenburg, Sweden

<sup>2</sup>Department of Electrical Engineering, Eindhoven University of Technology, 5612 AZ Eindhoven, The Netherlands

<sup>3</sup>NXP Semiconductors, 5656 AG Eindhoven, The Netherlands

Corresponding author: Navid Amani (anavid@chalmers.se)

This work was supported by the European Union's Horizon 2020 Research and Innovation Programme under Marie Skłodowska-Curie Grant 721732.

**ABSTRACT** A novel sparse automotive multiple-input multiple-output (MIMO) radar configuration is proposed for low-complexity super-resolution single snapshot direction-of-arrival (DOA) estimation. The physical antenna effects are incorporated in the signal model via open-circuited embedded-element patterns (EEPs) and coupling matrices. The transmit (TX) and receive (RX) array are each divided into two uniform sparse sub-arrays with different inter-element spacings to generate two MIMO sets. Since the corresponding virtual arrays (VAs) of both MIMO sets are uniform, the well-known spatial smoothing (SS) algorithm is applied to suppress the temporal correlation among sources. Afterwards, the co-prime array principle between two spatially smoothed VAs is deployed to avoid DOA ambiguities. A performance comparison between the sparse and conventional MIMO radars with the same number of TX and RX channels confirms a spatial resolution enhancement. Meanwhile, the DOA estimation error due to the mutual coupling (MC) is less pronounced in the proposed sparse architecture since antennas in both TX and RX arrays are spaced larger than half wavelength apart.

**INDEX TERMS** Automotive radar, DOA estimation, MIMO radar, mutual coupling, single snapshot, sparse arrays.

## I. INTRODUCTION

Automotive radars are becoming indispensable parts of autonomous vehicles and advanced driver assistant systems (ADASs). The radar angular resolution, which is inversely proportional to the array aperture size based on the well-known Rayleigh's criterion [1], is a critical factor to provide high-quality images. Since the number of transmit (TX) and receive (RX) channels are limited in practice, multiple-input multiple-output (MIMO) radars employing orthogonal waveforms have been widely deployed [2], [3]. This enables to virtually extend the aperture size and consequently

improve the radar angular resolution. Moreover, non-uniform sparse arrays, e.g., minimum redundancy arrays [4] and co-prime arrays [5], have been proposed to obtain more degrees-of-freedom (DOF).

Several challenges have to be overcome in automotive radars for precise direction-of-arrival (DOA) estimation. Critical constraints can be mentioned as (i) fine angular resolution, (ii) low latency, and (iii) low complexity [6], [7]. Traditional fast Fourier transform (FFT) based algorithm suffers from poor angular resolution [8]. Sub-space based techniques, e.g., multiple signal classification (MUSIC) [9] which relies on the estimate of the received signal covariance matrix, are proposed as super-resolution algorithms. Although MUSIC is independent of array geometry, it

The associate editor coordinating the review of this manuscript and approving it for publication was Luyu Zhao<sup>1</sup>.

performs unreliably when the number of snapshots (one radar measurement cycle) is smaller than the number of sources. The failure occurs due to the rank-deficiency of the covariance matrix. This is crucial in automotive applications since the low latency requirement demands for a single snapshot DOA estimation. Sparse sensor arrays equipped with sparse signal recovery algorithms, which deploys iterative [10] or probabilistic [11] approaches, are proposed to achieve a fine angular resolution using a single snapshot. Nonetheless, these methods are considered computationally heavy for real-time processing [12], [13]. Hence, a novel MIMO radar configuration for super-resolution single snapshot DOA estimation compatible with low complexity algorithms is highly desirable for the automotive industry.

In practical implementation, non-idealities such as mutual coupling (MC) between antenna elements and their impact on the DOA estimation need to be scrutinized. The MIMO radar principle requires the  $m$ -th orthogonal waveform to be transmitted by the  $m$ -th TX antenna. However, due to the MC, the  $m$ -th signal can be radiated by all transmitting antennas [14], [15]. Similarly, signals from all receiving antennas can contribute to the received signal by the  $n$ -th RX antenna. Hence, MC adjusts the array manifold of the virtual array (VA), which can potentially cause performance loss [15].

In this paper, a novel MIMO radar configuration with non-uniform sparse TX and RX arrays is proposed for super-resolution single snapshot DOA estimation in the presence of MC. The physical antenna effects are modeled through a diagonal matrix containing open-circuited embedded element patterns (EEPs) and a coupling matrix based on the impedance parameters. The TX and RX antennas are divided into two sub-arrays to generate two sets of MIMO radars, whose resultant VAs are sparse but uniform. Although both VAs suffer from aliasing due to spatial undersampling, a spatial smoothing (SS) algorithm [16] can be applied separately on each VA for correlation suppression of coherent sources. Afterwards, two spatially smoothed VAs from corresponding MIMO sets satisfy the co-primality concept, enabling us to resolve DOA ambiguities [5]. To the authors' best knowledge, this is the first time to propose a non-uniform sparse MIMO radar for single snapshot DOA estimation for which traditional FFT and sub-space based algorithms can be applied.

We first propose a generic signal model of a MIMO radar including physical antenna effects in Section II-A. In Section II-B a novel MIMO radar configuration with non-uniform sparse TX and RX arrays is presented. A case study with simulation results comparing conventional and proposed sparse MIMO radars is accomplished in Section III. Finally, conclusions are drawn in Section IV.

## II. SPARSE MIMO RADAR

### A. SIGNAL MODEL WITH COUPLED ANTENNAS

Assume  $K$  narrowband far-field sources located in the field-of-view (FoV) of a MIMO radar with  $M$  TX and  $N$  RX

antennas. The signal from the  $k$ -th source is denoted by  $s_k(t)$ . To generate a linear  $MN$ -element VA by the MIMO radar, waveform orthogonality and matched filtering at the TX and RX sides, respectively, are assumed to be perfect. Also, the TX and RX arrays are considered to be spaced several wavelengths apart, where there is no near-field coupling between these two arrays. Hence, the MC inside the TX and RX arrays can be modeled separately [15]. A received signal by an  $MN$ -element receive-only VA can therefore be represented by

$$\mathbf{x}(t) = \sum_{k=1}^K \mathbf{P}_k \mathbf{a}_k s_k(t) + \mathbf{n}(t), \quad t = 0, 1, 2, \dots \quad (1)$$

where  $\mathbf{a}_k = \mathbf{a}_k^T \otimes \mathbf{a}_k^R \in \mathbb{C}^{MN \times 1}$  is the steering vector of the VA due to the  $k$ -th source [2], [3].  $\mathbf{a}_k^T$  and  $\mathbf{a}_k^R$  are the TX and RX steering vectors denoted by superscripts  $T$  and  $R$ , respectively. The Kronecker product is denoted by  $\otimes$ . Commonly, array steering vectors are computed by the impractical assumption of isotropic radiators without MC. However, using realistic antennas the steering vectors are tailored by the physical antenna effects [14], [15], [17]. These effects are the element radiation pattern in the presence of other elements of an array, known as EEP, and mutual impedances between the elements. The antenna effects at both TX and RX arrays, affecting their corresponding steering vectors, can be incorporated in the signal model via the  $\mathbf{P}_k \in \mathbb{C}^{MN \times MN}$  matrix as

$$\mathbf{P}_k = (\mathbf{G}_k^T \mathbf{C}^T) \otimes (\mathbf{G}_k^R \mathbf{C}^R), \quad (2)$$

owing to the mixed-product property of the Kronecker product. The diagonal matrix  $\mathbf{G}$  of an array with  $\nu$  number of elements is

$$\mathbf{G} = \begin{bmatrix} \bar{G}_1^{\text{oc}}(\hat{r}_1) & 0 & \dots & 0 \\ 0 & \bar{G}_2^{\text{oc}}(\hat{r}_2) & \ddots & \vdots \\ \vdots & \ddots & \ddots & 0 \\ 0 & \dots & 0 & \bar{G}_\nu^{\text{oc}}(\hat{r}_\nu) \end{bmatrix}, \quad (3)$$

where the  $\nu$ -th open-circuited EEP, normalized by the antenna excitation current, is denoted by  $\bar{G}_\nu^{\text{oc}}(\hat{r}_\nu)$ <sup>1</sup> [18]. Depending on the  $k$ -th source direction, corresponding values of the EEPs form the  $\mathbf{G}_k$  matrix. The coupling matrix  $\mathbf{C}$  can be represented by impedance parameters as [19]

$$\mathbf{C} = (\mathbf{Z}_L + \mathbf{Z}_A)[\mathbf{Z}_L \mathbf{I} + \mathbf{Z}]^{-1}, \quad (4)$$

where  $\mathbf{Z}_L$  and  $\mathbf{Z}_A$  are the termination and isolated input impedances, respectively, and the array impedance matrix is denoted by  $\mathbf{Z}$ . The identity matrix is denoted by  $\mathbf{I}$ . Moreover,  $\mathbf{n}(t) \in \mathbb{C}^{MN \times 1}$  represents the receiver complex Gaussian noise satisfying  $\mathbf{n} \sim \mathcal{CN}(\mathbf{0}, \sigma^2 \mathbf{I})$ , where  $\sigma^2$  is the noise power.

<sup>1</sup>Field vectors are represented by overbar ( $\bar{G}$ ), while boldface upper case and lower case denotes matrices and vectors, respectively.

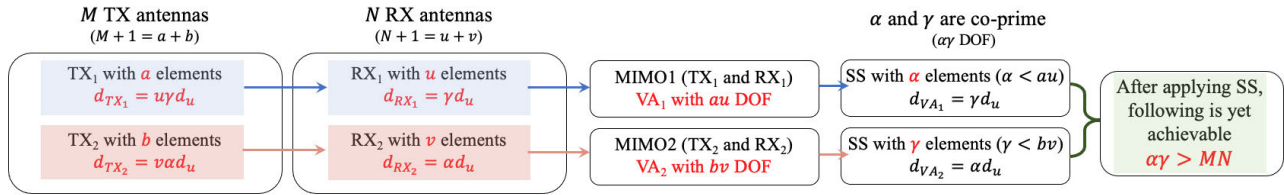


FIGURE 1. Sparse MIMO radar principle for single snapshot DOA estimation with an enhanced angular resolution.

### B. NON-UNIFORM TX AND RX ARRAY CONFIGURATIONS

Traditionally, a MIMO radar configuration requires a widely-spaced TX array and a conventional RX array with  $0.5\lambda$  inter-element spacing [2], where  $\lambda$  is a wavelength. With the aid of waveform orthogonality, an anti-aliasing uniform VA with  $0.5\lambda$  inter-element spacing is achievable. To further improve the angular resolution, a uniform sparse VA with an element spacing larger than half-wavelength can be realized. However, its major drawback known as aliasing occurs. In order to address the aliasing issue, the same number of  $M$  TX and  $N$  RX elements can form two sets of uniform sparse MIMO radars. The underlying reason to maintain uniformity is to be able to apply the SS algorithm for correlation suppression. Since both MIMO sets suffer from aliasing problems, the physical elements need to be positioned in a new arrangement so that the VAs of two MIMO sets become co-prime. Therefore, aliasing can be addressed by comparing the spectra achieved by the two MIMO sets and selecting overlapping peaks as true source directions.

When  $M > 2$  or  $N > 2$ , the radar angular resolution can be enhanced by dividing the TX and RX arrays into two uniform sub-arrays with different inter-element spacings. This renders TX<sub>1</sub>, TX<sub>2</sub>, RX<sub>1</sub>, and RX<sub>2</sub> arrays. Assuming that TX<sub>1</sub> and TX<sub>2</sub> with  $a$  and  $b$  number of elements, respectively, are sharing one element,  $M+1 = a+b$  holds. Similarly,  $N+1 = u+v$  holds for RX<sub>1</sub> and RX<sub>2</sub> with  $u$  and  $v$  number of elements, respectively. Then, TX<sub>1</sub> and RX<sub>1</sub> arrays form the MIMO1 set, where the MIMO2 set is comprised of TX<sub>2</sub> and RX<sub>2</sub> arrays. Although both MIMO sets are comprised of uniform sparse sub-arrays, the total TX and RX arrays are non-uniform.

The corresponding uniform sparse VAs from the two MIMO sets have  $au$  and  $bv$  number of elements which are both smaller than  $MN$ . However, if two VAs satisfy the co-primality concept, the angular resolution of an array with  $(au \times bv)$ -elements can be reached, which satisfies  $(au \times bv) > MN$ . This indicates that more DOF can be reached. To this end, the number of elements in the two VAs, which are  $au$  and  $bv$ , have to be co-prime. Meanwhile, the element spacing in each VA needs to be computed by the number of elements in the other VA multiplied by the unit spacing  $d_u = 0.5\lambda$ . This arrangement assures that the grating lobes of VAs are not overlapping [5]. Hence, the DOA ambiguities from each VA can be resolved by comparing two spectra.

For the super-resolution DOA estimation algorithms, e.g., MUSIC [9], the covariance matrix of the received signal is needed. That is

$$\mathbf{R}_{xx} = \mathbb{E}\{\mathbf{x}(t)\mathbf{x}^H(t)\}, \quad (5)$$

where  $\mathbb{E}$  and  $(\cdot)^H$  represent the expectation and Hermitian operators, respectively. Commonly, the expectation is approximated by time averaging using several snapshots. However, when the number of snapshots is limited the well-known SS algorithm selects similar overlapping sub-arrays within a uniform array and performs spatial averaging over the number of sub-arrays [16]. Since length of sub-arrays (LSAs) is smaller than the whole uniform array, the SS algorithm causes an angular resolution loss as its major drawback. However, its simplicity is the underlying reason for its widespread usage in practice. In the proposed MIMO radar configuration, the SS can be applied separately on each VA since they are uniform. Assume that the SS algorithm selects sub-arrays with  $\alpha$  number of elements in VA1 and  $\gamma$  number of elements in VA2. The two spatially smoothed VAs with  $\alpha$  and  $\gamma$  number of elements, need to satisfy the co-primality principle to avoid ambiguity. The proposed solution enables a single snapshot DOA estimation of a limited number of sources with enhanced DOF. That is,  $\alpha\gamma > MN$ . The overall principle of the proposed non-uniform sparse MIMO radar is summarized in Fig. 1.

It is worth noting that, the proposed approach is in contrast to the previous studies combining MIMO and co-prime concepts [20], [21]. In such studies, a difference co-array is first generated and afterwards the SS algorithm is applied, which is valid with the assumption of uncorrelated sources. With a single snapshot availability, when sources become coherent, generating a difference co-array by vectorization of the covariance matrix is erroneous [22].

## III. NUMERICAL SIMULATIONS

### A. CASE STUDY AND OPERATION MECHANISM

Fig. 2(a) is the schematic representation of the proposed sparse MIMO radar configuration with  $M = 6$  and  $N = 5$ . The number of elements in uniform TX<sub>1</sub>, TX<sub>2</sub>, RX<sub>1</sub>, and RX<sub>2</sub> sub-arrays are selected as  $a = 4$ ,  $b = 3$ ,  $u = 3$ , and  $v = 3$ , respectively. The element indices per sub-array are:  $i_{TX_1} = \{1, 2, 4, 6\}$ ,  $i_{RX_1} = \{1, 2, 4\}$ ,  $i_{TX_2} = \{1, 3, 5\}$ , and  $i_{RX_2} = \{1, 3, 5\}$ . Therefore, the MIMO1 radar creates the VA1 with 12 elements, while the MIMO2 generates the

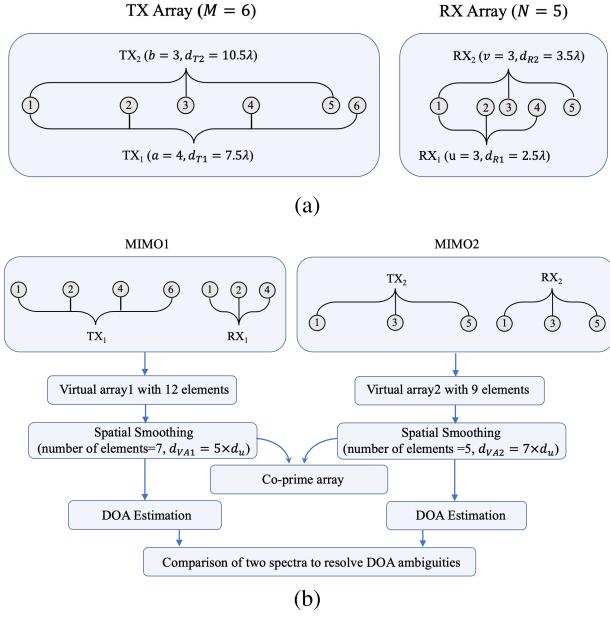


**FIGURE 2.** Sparse MIMO radar configuration (a) with non-uniform TX and RX arrays; (b) two MIMO sets and signal processing steps for an enhanced DOA estimation.

VA2 with 9 elements. We assume the availability of a single snapshot. In the SS algorithm, the sub-arrays are assumed to have 7 elements for VA1 and 5 elements for VA2, which are co-prime numbers.

A bottom-up design flow is followed in Fig. 2(b) to calculate the element spacings in TX1, TX2, RX1 and RX2 sub-arrays. Based on the co-primality design principle, the element spacing in VA1 needs to be  $d_{VA1} = 5 \times d_u = 2.5\lambda$ , since the number of elements in VA2 after applying the SS algorithm is 5. Similarly, the element spacing in VA2 is computed by  $d_{VA2} = 7 \times d_u = 3.5\lambda$ . The element spacings in RX1 and RX2 are  $d_{VA1}$  and  $d_{VA2}$ , respectively. Based on the MIMO radar concept, the element spacing in the TX array is computed by the RX element spacing multiplied by the number of elements in the RX array. Therefore,  $d_{T1} = u \times d_{R1} = 7.5\lambda$  and  $d_{T2} = v \times d_{R2} = 10.5\lambda$ .

The array steering vector of the  $(6 \times 5)$ -element array due to the  $k$ -th source, including physical antenna effects, is  $\mathbf{P}_k \mathbf{a}_k \in \mathbb{C}^{30 \times 1}$ . The steering vectors of the two VAs by the MIMO1 and MIMO2 sets need to be extracted from  $\mathbf{P}_k \mathbf{a}_k$  by a proper row selection based on the element indices. The corresponding row indices can be computed by

$$\begin{cases} R1 = [(i_{TX1} - 1) \times N] + i_{RX1} & \text{for VA1} \\ R2 = [(i_{TX2} - 1) \times N] + i_{RX2} & \text{for VA2.} \end{cases} \quad (6)$$

Therefore,  $R1 = \{1, 2, 4, 6, 7, 9, 16, 17, 19, 26, 27, 29\}$  represents the row indices of  $\mathbf{P}_k \mathbf{a}_k$ , which form the steering vector of the VA1. Likewise,  $R2 = \{1, 3, 5, 11, 13, 15, 21, 23, 25\}$  contains the row indices which cast the steering vector of the VA2. Afterwards, the received signal vectors by VA1 and VA2 are calculated.

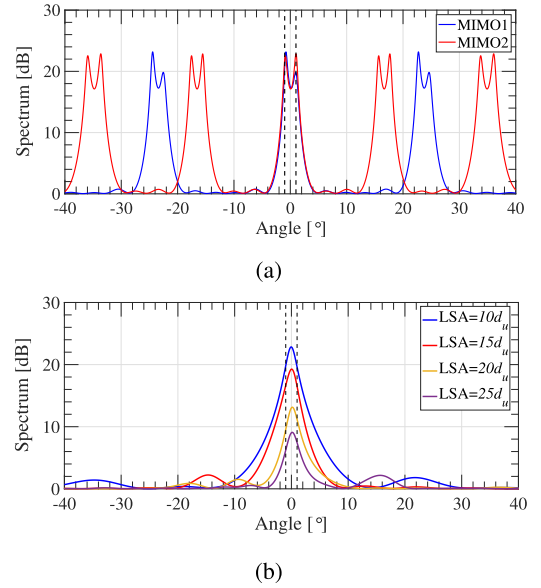


**FIGURE 3.** Single-snapshot DOA estimation of two sources located at  $-1^\circ$  and  $+1^\circ$ , shown by dashed black lines, and SNR = 10 dB using the (a) proposed sparse MIMO radar; (b) conventional MIMO radar with different sub-array lengths in the SS algorithm.

For simplicity the physical antenna effects are neglected in this sub-section, hence  $\mathbf{P}_k = \mathbf{I}$  is assumed. We consider two equal-power sources with  $2^\circ$  angular separation located at  $[-1^\circ, +1^\circ]$ , shown by black dashed lines in Fig. 3. The SNR per source is assumed to be 10 dB. The MUSIC algorithm is applied for the DOA estimation after applying the SS algorithm separately on each VA. Fig. 3(a) demonstrates the spectra achieved by the proposed sparse MIMO radar. It can be seen that the peaks of the two spectra at the source directions overlap, while the rest do not. Fig. 3(a) confirms that the proposed sparse MIMO radar can successfully distinguish two close-by sources with  $2^\circ$  angular separation.

In the conventional MIMO radar with  $M = 6$  and  $N = 5$ , where the element spacing in the RX array is  $d_u = 0.5\lambda$ , the TX elements are spaced by  $2.5\lambda$ . Its corresponding VA is therefore a 30-element uniform linear array with  $0.5\lambda$  element spacing. For the same scenario, two sources with  $2^\circ$  angular separation cannot be distinguished using a conventional MIMO radar when different LSAs are used in the SS algorithm, as shown in Fig. 3(b).

## B. PERFORMANCE COMPARISON WITH COUPLED ANTENNAS

In this sub-section, half-wavelength vertically oriented resonant wire dipoles are used as antenna elements of both conventional and sparse MIMO radars. In order to incorporate the physical antenna effects, full-wave simulations are carried out in CST Microwave Studio [23]. The isolated input impedance of the thin dipoles with radius  $r = 10^{-3}\lambda$  at 77 GHz is computed as  $Z_A = 87.23 + j59.72$ . For a maximum power

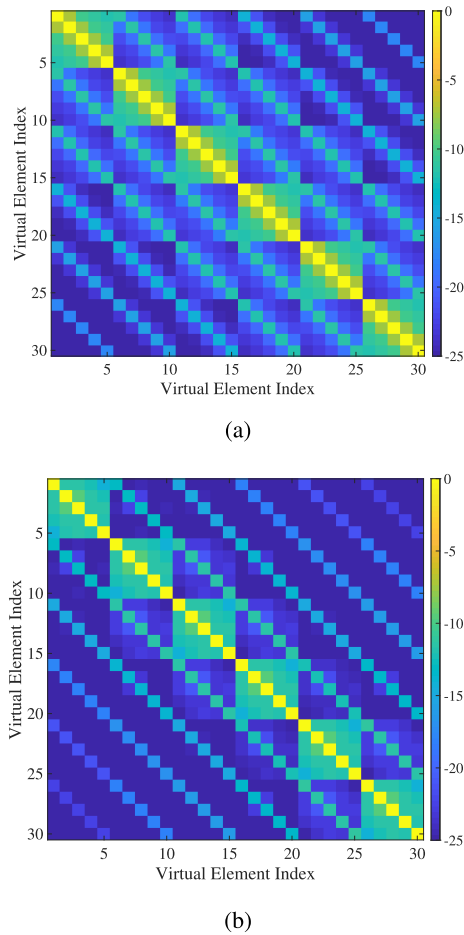


**FIGURE 4.** Mutual coupling matrix of (a) conventional; (b) sparse; MIMO radar configurations.

transfer,  $Z_L$  is assumed to be the complex conjugate of the  $Z_A$ . Open-circuited thin dipoles spaced sufficiently apart can be approximated as minimum scattering antennas [24]. Hence, due to the omni-directional radiation pattern of dipoles in the horizontal plane and taking into account that sources are assumed to be located in this plane,  $\mathbf{G} = \mathbf{I}$  are used in (2) for both TX and RX arrays. The impedance matrices of the TX and RX array are extracted from CST and afterwards the coupling matrices  $\mathbf{C}$  are calculated through (4). A comparison between the coupling matrices of the conventional and sparse MIMO radars, shown in Fig. 4, demonstrates lower values for off-diagonal elements by the sparse configuration. This interprets as reduced MC by the proposed configuration due to the sparsity.

Similar to the previous sub-section, for the proposed MIMO architecture the steering vectors of VAs are extracted from  $\mathbf{P}_k \mathbf{a}_k$ . Afterwards, the SS and the DOA estimation algorithms are applied on each VA. Due to the residual error in the estimation algorithm, peaks of the two spectrums at source directions are not exactly overlapping. Hence, all peaks inside the FoV from the two spectrums are found and those with

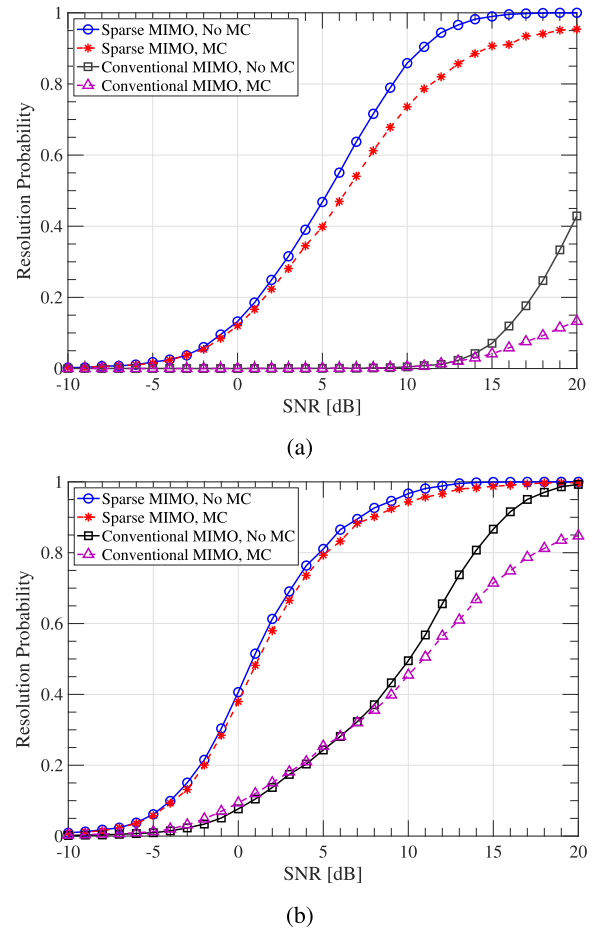


**FIGURE 5.** Resolution probability of sparse and conventional MIMO radars with and without MC for two sources with angular separation of (a) 2°; (b) 3°.

minimum angular differences are selected as the true source directions [25]. For the conventional MIMO configuration,  $LSA = 20d_u$  is used. In a Monte Carlo simulation, the DOA estimation is performed  $10^4$  times for two equi-power sources. In each simulation run, the first source location is determined stochastically based on the uniform probability density function (pdf). The second source is located with a fine and constant angular separation from the first source inside the  $FoV = 80^\circ$ . The actual source angles are denoted by  $\theta$ , while  $\hat{\theta}$  represents the estimated angles. The error of DOA estimation is computed as

$$\epsilon = \left[ \sum_{k=1}^K (\theta_k - \hat{\theta}_k)^2 \right]^{\frac{1}{2}}. \quad (7)$$

A DOA estimation is considered to be successful when  $K$  sources are found and  $\epsilon \leq K$ . Afterwards, the resolution probability is calculated as the rate of successful DOA estimation over the total number of simulation runs.

The resolution probability achieved by the proposed and conventional MIMO radars for 2° and 3° angular separations

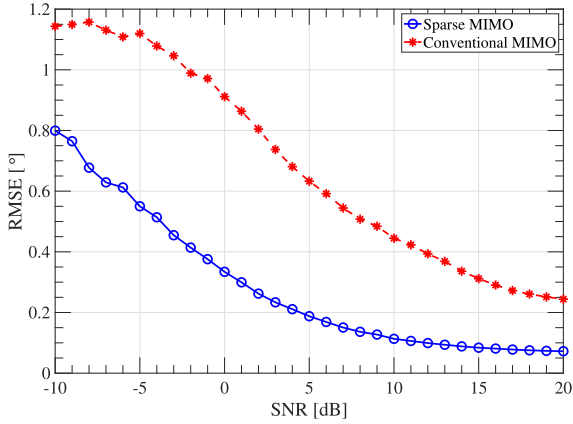


**FIGURE 6.** RMSE versus different SNR values, in the presence of MC, for single snapshot DOA estimation of two targets located at  $-1.5^\circ$  and  $1.5^\circ$ .

between two sources versus SNR are computed and plotted in Fig. 5(a) and (b), respectively. The MC effects between dipoles on the DOA estimation performance are also examined. The spatial resolution of the proposed sparse MIMO radar is significantly enhanced with respect to the conventional MIMO radar. This confirms the superior capability of the proposed sparse MIMO configuration to distinguish close-by sources. The MC effect in the lower SNR regime, where the resolution probability is quite low, is negligible for both MIMO radar configurations. However, for higher SNR values the MC is seen to be degrading for the DOA estimation performance, which certifies the necessity of calibration methods. It is worth noting that, the adverse effect of MC is less pronounced in the proposed MIMO configuration. That is due to the sparsity in both TX and RX arrays of the proposed MIMO radar, where in the conventional MIMO radar only the TX array elements are spaced further than  $0.5\lambda$ .

For the cases that the DOA estimation is considered successful, the root mean square error (RMSE) is computed by:

$$\text{RMSE} = \sqrt{\frac{1}{L_0 K} \sum_{i=1}^{L_0} \sum_{k=1}^K \left[ (\theta_k - \hat{\theta}_k^i)^2 \right]}, \quad (8)$$

where  $L_0 = 5000$  is the number of Monte Carlo trials. Two close-by targets are assumed to be located at  $-1.5^\circ$  and  $1.5^\circ$ . The RMSE curves for different SNR values, in the presence of MC, from successful single snapshot DOA estimation are plotted in Fig. 6. Lower RMSE values by the sparse MIMO radar confirms that it achieves a better angular resolution in comparison with the conventional MIMO radar.

In order to examine the performance of the proposed MIMO radar in case of multiple simultaneous sources, even more than two, a Monte Carlo simulation is conducted for a fixed SNR value and constant angular separations among sources. The resolution probability is computed, including MC, in the same way as in Fig. 5, when the number of

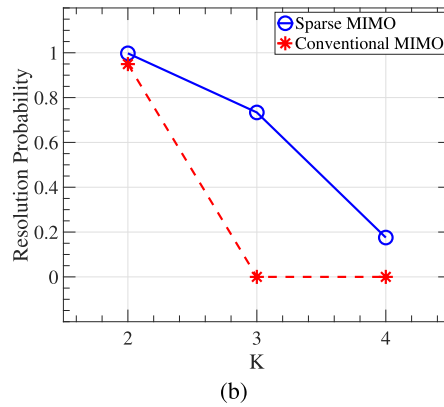
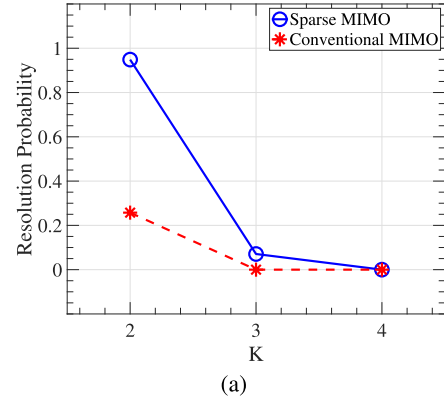


**FIGURE 7.** Resolution probability for different number of sources achieved by sparse and conventional MIMO radars, including MC, for SNR = 20dB per source and constant angular separations of (a)  $2^\circ$ ; and (b)  $3^\circ$ .

sources increases from two to four. As expected, the larger the number of sources, the more challenging the DOA estimation. Constant angular separations of  $2^\circ$  and  $3^\circ$  are considered among sources. The SNR per source is assumed to be 20 dB. As can be observed in Fig. 7, the angular resolvability is enhanced by the proposed sparse MIMO configuration, in contrast to its conventional counterpart. The sparse MIMO radar demonstrates the superior capability of distinguishing a limited number of sources with fine angular separation and a single snapshot availability.

#### IV. CONCLUSION

A novel MIMO radar configuration has been presented by array sparsity at both TX and RX arrays for a low-complexity super-resolution DOA estimation. In spite of non-uniform distribution of elements, the SS algorithm can be applied by generating two uniform MIMO sets, which are co-prime. The co-primality concept prevents DOA ambiguities. This has made the proposed solution suitable for automotive applications, where the number of snapshots is limited. A generic signal model including physical antenna effects has been introduced. It has been observed that the MC effects are less degrading in the proposed sparse MIMO radar, compared to

the conventional MIMO configuration. Meanwhile, superior angular resolvability has been achieved by the sparse MIMO radar.

## REFERENCES

- [1] J. Hatch, A. Topak, R. Schnabel, T. Zwick, R. Weigel, and C. Waldschmidt, "Millimeter-wave technology for automotive radar sensors in the 77 GHz frequency band," *IEEE Trans. Microw. Theory Techn.*, vol. 60, no. 3, pp. 845–860, Mar. 2012.
- [2] E. Fishler, A. Haimovich, R. Blum, D. Chizhik, L. Cimini, and R. Valenzuela, "MIMO radar: An idea whose time has come," in *Proc. IEEE Radar Conf.*, Apr. 2004, pp. 71–78.
- [3] F. C. Robey, S. Coutts, D. Weikle, J. C. McHarg, and K. Cuomo, "MIMO radar theory and experimental results," in *Proc. 28th Asilomar Conf. Signals, Syst. Comput.*, Nov. 2004, pp. 300–304.
- [4] A. Moffet, "Minimum-redundancy linear arrays," *IEEE Trans. Antennas Propag.*, vol. AP-16, no. 2, pp. 172–175, Mar. 1968.
- [5] P. P. Vaidyanathan and P. Pal, "Sparse sensing with co-prime samplers and arrays," *IEEE Trans. Signal Process.*, vol. 59, no. 2, pp. 573–586, Feb. 2011.
- [6] Y.-C. Lin and T.-S. Lee, "Max-music: A low-complexity high-resolution direction finding method for sparse MIMO radars," *IEEE Sensors J.*, vol. 20, no. 24, pp. 14914–14923, Dec. 2020.
- [7] P. H  cker and B. Yang, "Single snapshot DOA estimation," *Adv. Radio Sci.*, vol. 8, pp. 251–256, Oct. 2010.
- [8] P. J. Chung, "DOA estimation methods and algorithms," in *Academic Press Library in Signal Processing*, vol. 3. Amsterdam, The Netherlands: Elsevier, 1994, pp. 599–650.
- [9] R. O. Schmidt, "Multiple emitter location and signal parameter estimation," *IEEE Trans. Antennas Propag.*, vol. AP-34, no. 3, pp. 276–280, Mar. 1986.
- [10] F. Roos, P. Hugler, L. L. T. Torres, C. Knill, J. Schlichenmaier, C. Vasanelli, N. Appenrodt, J. Dickmann, and C. Waldschmidt, "Compressed sensing based single snapshot DoA estimation for sparse MIMO radar arrays," in *Proc. 12th German Microw. Conf. (GeMiC)*, Mar. 2019, pp. 75–78.
- [11] A. A. Hilli and A. Petropulu, "MIMO radar using sparse sensing: A weighted sparse Bayesian learning (WSBL) approach," in *Proc. 51st Asilomar Conf. Signals, Syst., Comput.*, Oct. 2017, pp. 80–84.
- [12] C. Waldschmidt, J. Hasch, and W. Menzel, "Automotive radar—From first efforts to future systems," *IEEE J. Microw.*, vol. 1, no. 1, pp. 135–148, Jan. 2021.
- [13] F. Roos, P. H  gler, J. Bechter, M. A. Razzaq, C. Knill, N. Appenrodt, J. Dickmann, and C. Waldschmidt, "Effort considerations of compressed sensing for automotive radar," in *Proc. IEEE Radio Wireless Symp.*, Jan. 2019, pp. 1–3.
- [14] B. Friedlander and A. Weiss, "Direction finding in the presence of mutual coupling," *IEEE Trans. Antennas Propag.*, vol. 39, no. 3, pp. 273–284, Mar. 1991.
- [15] B. T. Arnold and M. A. Jensen, "The effect of antenna mutual coupling on MIMO radar system performance," *IEEE Trans. Antennas Propag.*, vol. 67, no. 3, pp. 1410–1416, Mar. 2019.
- [16] T.-J. Shan, M. Wax, and T. Kailath, "On spatial smoothing for direction-of-arrival estimation of coherent signals," *IEEE Trans. Acoust., Speech, Signal Process.*, vol. ASSP-33, no. 4, pp. 806–811, Apr. 1985.
- [17] A. Durr, D. Schwarz, F. Roos, P. Hugler, S. Bucher, P. Gr  ner, and C. Waldschmidt, "On the calibration of mm-wave MIMO radars using sparse antenna arrays for DoA estimation," in *Proc. 49th Eur. Microw. Conf. (EuMC)*, Oct. 2019, pp. 349–352.
- [18] P.-S. Kildal, *Foundations of Antenna Engineering: A Unified Approach for Line-of-Sight and Multipath*. Norwood, MA, USA: Artech House, 2015.
- [19] B. Clerckx, C. Craeye, D. Vanhoenacker-Janvier, and C. Oestges, "Impact of antenna coupling on  $2 \times 2$  MIMO communications," *IEEE Trans. Veh. Technol.*, vol. 56, no. 3, pp. 1009–1018, May 2007.
- [20] J. Shi, G. Hu, X. Zhang, F. Sun, W. Zheng, and Y. Xiao, "Generalized co-prime MIMO radar for DOA estimation with enhanced degrees of freedom," *IEEE Sensors J.*, vol. 18, no. 3, pp. 1203–1212, Feb. 2018.
- [21] J. Shi, F. Wen, and T. Liu, "Nested MIMO radar: Coarrays, tensor modeling, and angle estimation," *IEEE Trans. Aerosp. Electron. Syst.*, vol. 57, no. 1, pp. 573–585, Feb. 2021.
- [22] A. Koochakzadeh and P. Pal, "Exact localization of correlated sources using 2D harmonics retrieval," in *Proc. 50th Asilomar Conf. Signals, Syst. Comput.*, Nov. 2016, pp. 1503–1507.
- [23] Computer Simulation Technology. (2018). *CST Microwave Studio 2018*. [Online]. Available: <https://www.cst.com/>
- [24] C. Craeye and D. Gonz  lez-Ovejero, "A review on array mutual coupling analysis," *Radio Sci.*, vol. 46, no. 2, pp. 1–25, 2011.
- [25] C. Zhou, Z. Shi, Y. Gu, and X. Shen, "DECOM: DOA estimation with combined MUSIC for coprime array," in *Proc. Int. Conf. Wireless Commun. Signal Process.*, Oct. 2013, pp. 1–5.



**NAVID AMANI** received the M.Sc. degree in telecommunication engineering from the K. N. Toosi University of Technology, Tehran, Iran, in 2013. He is currently pursuing the Ph.D. degree with the Chalmers University of Technology, Gothenburg, Sweden, as a Marie Sk  łodowska-Curie Actions (MSCA) Fellow, investigating novel array architectures for 5G MU-MIMO. From 2013 to 2015 and from 2016 to 2017, he was with the Electromagnetic and Antenna (EMA) Laboratory, Amirkabir University of Technology, Tehran, where he was involved in metamaterials for antenna applications. In 2017, he was a Visiting Researcher at ASTRON, the Netherlands Institute for Radio Astronomy, Dwingeloo, The Netherlands. During his Ph.D., he is also collaborating with the Electromagnetics Group, Eindhoven University of Technology (TU/e), and NXP Semiconductors, Eindhoven, The Netherlands. His research interests include antenna arrays, array signal processing, MU-MIMO communication, and MIMO radar.



**FEIKE JANSEN** was born in Eindhoven, The Netherlands, in 1980. He received the M.Sc. degree in electrical engineering from the Technical University of Eindhoven, Eindhoven, in 2006. In 2006, he joined Philips N.V., as a Researcher in the field of 24 GHz radar antennas. In 2007, he joined NXP Semiconductors N.V., where he is currently working as the Principal Scientist with the Algorithms and Software Innovation Group. There he worked on algorithm develop-

ment for 60 GHz wireless communication basebands. Since several years, he has been working on algorithms and system design for 79 GHz automotive radar systems.



**ALESSIO FILIPPI** (Member, IEEE) graduated in telecommunication engineering from the University of Padova, Italy, in 2002. From 2001 to 2004, he was with Siemens in Munich, Germany. While at Siemens, he pursued his Ph.D. at the Technical University of Kaiserslautern under the supervision of Professor P. W. Baier. In 2005, he joined Philips Research in the Netherlands and obtained his doctoral degree. His research interests include modulation and demodulation techniques for wireless communications, with a focus on synchronization and channel estimation algorithms for multi-carrier systems.



**MARIANNA V. IVASHINA** (Senior Member, IEEE) received the Ph.D. degree in electrical engineering from the Sevastopol National Technical University (SNTU), Ukraine, in 2001. From 2001 to 2010, she was with ASTRON, the Netherlands Institute for Radio Astronomy, where she carried out research on innovative phased array technologies for future radio telescopes, such as the square kilometer array (SKA). From 2002 to 2003, she also stayed as a Visiting

Scientist with the European Space Agency (ESA), ESTEC, where she studied multiple-beam array feeds for the satellite telecommunication system large deployable antennas (LDA). In January 2011, she joined the Chalmers University of Technology, Gothenburg, Sweden, where she is currently a Full Professor and the Head of the Antenna Systems Group, Department of Electrical Engineering. Her current research interests include antenna array systems, integration of antennas with active electronic components, synthesis of aperiodic arrays and other unconventional array architectures, reflector antennas, and focal plane array feeds. She has published extensively on the above topics, having authored/coauthored over 130 journal articles and conference papers. She is a Board Member of the European School of Antennas (ESoA). She has received several scientific awards, including the URSI Young Scientists Award for GA URSI, Toronto, Canada, in 1999, the APS/IEEE Travel Grant, Davos, Switzerland, in 2000, the Best Team Contribution Paper Award at the ESA Antenna Workshop, in 2008, the EU FP7 Marie Curie Actions International Qualification Fellowship, in 2009, the Best Paper Award at the IEEE COMCAS Conference, Tel-Aviv, Israel, in 2019, and numerous research project funding grants from Swedish and European funding agencies. She is an Associate Editor of the IEEE TRANSACTIONS ON ANTENNAS AND PROPAGATION.



**ROB MAASKANT** (Senior Member, IEEE) received the M.Sc. and Ph.D. degrees (*cum laude*) in electrical engineering from the Eindhoven University of Technology (TU/e), Eindhoven, The Netherlands, in 2003 and 2010, respectively. He was an Antenna Researcher with the Netherlands Institute for Radio Astronomy, Dwingeloo, The Netherlands, from 2002 to 2010. Since 2010, he has been with the Antenna Group, Signals and Systems Department, Chalmers Uni-

versity of Technology, Gothenburg, Sweden, where he held a postdoctoral position, and was also an Assistant Professor. He is currently an Associate Professor with the Chalmers University of Technology and TU/e. The latter position is owing to a five-year Vidi Grant from the Dutch Research Council. He is the primary author of the CAESAR software, an advanced integral equation-based solver for the analysis of large antenna array systems. His current research interest includes the analysis and design of integrated antenna array systems for future wireless applications. He has served the AP Community as an Associate Editor for the IEEE TRANSACTIONS ON ANTENNAS AND PROPAGATION and the IEEE ANTENNAS AND WIRELESS PROPAGATION LETTERS. He is on the Editorial Board of a unique open-access journal *Forum for Electromagnetic Research Methods and Application Technologies* (<http://www.e-fermat.org>).

...